ISSN 1063-7788, Physics of Atomic Nuclei, 2010, Vol. 73, No. 11, pp. 1956–1962. © Pleiades Publishing, Ltd., 2010.
Original Russian Text © R.A. Ryutin, 2010, published in Yadernaya Fizika, 2010, Vol. 73, No. 11, pp. 2009–2015.

ELEMENTARY PARTICLES AND FIELDS
Theory

Investigation of Diffractive Processes with the CMS Detector: New Results

R. A. Ryutin*

Institute for High Energy Physics, Protvino, Moscow oblast, 142284 Russia

Received March 3, 2010

Abstract—An experiment aimed at studying leading neutrons at LHC with the aid of the CMS detectors is proposed. Data of this experiments can be used to extract cross sections for π^+p and $\pi^+\pi^+$ scattering. Numerical estimates are presented for the proposed measurements.

DOI: 10.1134/S1063778810110207

1. INTRODUCTION

On the basis of a phenomenological analysis, one can state that diffractive processes are responsible for a significant part of total cross sections at energies in excess of several TeV units. For LHC, the respective predicted values range between 15 and 25%. Single diffraction (SD), double diffraction (DD), and central diffraction (CD) are dominant diffractive processes. As is well known, gaps in the rapidity distribution of particles and small (not greater than 10%) longitudinal losses of momenta of colliding hadrons are among the main signatures of diffractive processes.

There is a diffractive-physics working group in the CMS Collaboration. The main processes studied by this group include (i) jet production ($p + p \to N^* + jjX$, where N^* is a proton or hadron-dissociation products, jj stands for jets, and "+" denotes rapidity gaps) and W-boson production ($p + p \to N^* + W(\to \mu\nu)X$) studied in hard single diffraction [1, 2] in order to measure diffraction structure functions and corrections associated with rescattering; (ii) exclusive lepton production [3] ($p + p \to p + l^+l^- + p$ through $\gamma\gamma \to l^+l^-$ and $\gamma p \to \Upsilon \to l^+l^-$) studied in order to measure the luminosity and to perform detector calibrations; and (iii) inclusive jet production $p + p \to j + X$ and forward-jet (so-called Mueller–Navelet jets) production $p + p \to j_1 + j_2$ studied in order to test perturbative QCD, to obtain constraints on parton distributions, and to verify the Balitsky–Fadin–Kuraev–Lipatov (BFKL) evolution [4].

The exclusive-central-diffraction (ECD) process $p + p \to p + M_c + p$, where M_c is a central system, plays a particularly important role. Calculations of the cross sections for this process can be found in [5–10]. The advantages of the ECD process are known to include (i) a clear-cut signature consisting in the presence of two final-state protons, a central system whose decay products are recorded by the CMS detectors, and two rapidity gaps; (ii) a large value of the signal-to-background ratio owing to the exclusive character of the process; (iii) a high resolution in the mass of the central system and the possibility of employing the missing-mass method; and (iv) the possibility of performing a spin-parity analysis in the azimuthal distribution of final-state protons [7]. However, there is a flaw: ECD cross sections are small, which requires a long-term accumulation of statistics. The presence of a large number of pileup events at high luminosities, which are required for a fast accumulation of statistics, stands out among experimental difficulties. Investigations into ECD processes are motivated primarily by (a) the possibility of observing the production of various heavy states predicted by the Standard Model and its extensions (for example, the Higgs boson, two or three high-transverse-momentum jets, gauge bosons, gravitons, glueballs, and superpartners) and determining their quantum numbers via a spin–parity analysis and (b) the possibility of tracing the evolution of the diffraction pattern [9] versus the hard scale (derivation of information about the strength of the interaction and about the shape and size of the interaction region).

There is yet another interesting possibility for diffractive investigations with CMS. It consists in detecting leading neutrons and in extracting cross sections for π^+p and $\pi^+\pi^+$ scattering. This possibility is associated with the leading contribution of pion exchange at low momentum transfers. Here, physical interest consists primarily in obtaining pion–proton and pion–pion cross sections at energies of several TeV units [11]. While pion–proton cross

*E-mail: Roman.Rioutine@cern.ch

sections are known to energies of several tens of GeV units, pion–pion cross sections are known only to energies of several GeV units. There arises the possibility of studying the entire set of problems associated with the behavior of cross sections and their ratios at high energies. These include the problem of determining the energy at which the cross sections begin growing and the question of whether all cross sections tend to the same limit independent of the colliding-particle type. In this article, we present the results of calculations for the case of extracting total and elastic cross sections.

2. NEW RESULTS: LHC AS πp AND $\pi\pi$ COLLIDER

2.1. Theory

The possibility of extracting the total cross sections for $\pi^+ p$ and $\pi^+\pi^+$ scattering in single- and double-charge-exchange processes was recently studied in [11]. At low squares of the momentum transfer ($|t_i| < 0.5$ GeV^2), a dominant contribution to these processes comes from single (SπE) and double (DπE) pion exchanges. The ρ- and a_2-meson contributions are smaller by 20% in the t region studied here [12], and we can readily take them into account.

The kinematics of pion exchanges is illustrated in Fig. 1. The cross sections for the processes being considered are estimated by the formulas [11]

$$\frac{d\sigma_{\mathrm{S}\pi\mathrm{E}}}{d\xi dt} = [E(t,\xi)S(s/s_0,\xi,t)]\,\sigma_{\pi^+p}(\xi s), \quad (1)$$

$$\frac{d\sigma_{\mathrm{D}\pi\mathrm{E}}}{d\xi_1 d\xi_2 dt_1 dt_2} \quad (2)$$
$$= [E(t_1,\xi_1)E(t_2,\xi_2)S_2(s/s_0,\{\xi_i\},\{t_i\})] \times \sigma_{\pi^+\pi^+}(\xi_1\xi_2 s),$$

$$E(t,\xi) = \frac{G^2_{\pi^+pn}}{16\pi^2}\frac{-t}{(t-m_\pi^2)^2}F^2(t)\xi^{1-2\alpha_\pi(t)}, \quad (3)$$

where $G^2_{\pi^+pn}/(8\pi) = 13.75$ [13], ξ and ξ_i are the primary-proton-longitudinal-momentum fractions carried away by pions, and the pion trajectory is determined by the expression

$$\alpha_\pi(t) = 0.9(t - m_\pi^2). \quad (4)$$

The form factor $F(t)$ is usually represented in an exponential form,

$$F(t) = \exp(bt), \quad (5)$$

where it is assumed that $b \simeq 0.3$ GeV^{-2}, which is suggested by recent experimental data from [12, 14]. We are interested in the kinematical region specified by the inequalities $0.01 < |t| < 0.5$ GeV^2 and $\xi <$ 0.4, where Eqs. (1) and (2) are valid [15, 16]. In order to estimate the cross sections at high energies, we can employ any adequate parametrizations of the cross sections for $\pi^+ p$ and $\pi^+\pi^+$ scattering [17–21]. The absorptive corrections S and S_2, which are associated with initial-state (final-state) rescattering, were calculated in [11] on the basis of the three-Pomeron Regge–eikonal model [22] featuring the trajectories

$$\alpha_{IP_1}(t) - 1 = (0.0578 \pm 0.002) + (0.5596 \pm 0.0078)t, \quad (6)$$
$$\alpha_{IP_2}(t) - 1 = (0.1669 \pm 0.0012) + (0.2733 \pm 0.0056)t,$$
$$\alpha_{IP_3}(t) - 1 = (0.2032 \pm 0.0041) + (0.0937 \pm 0.0029)t.$$

These trajectories are the result of a 20-parameter description of data on the total and differential cross sections for pp and $p\bar{p}$ scattering in the region specified by the equation

$$0.01 < |t| < 14 \text{ GeV}^2, \quad (7)$$

$$8 < \sqrt{s} < 1800 \text{ GeV}. \quad (8)$$

Although the value of χ^2/d.o.f. $= 2.74$ is quite large, the model yields good predictions for the total and elastic cross sections (χ^2/d.o.f. ~ 1 in the small-t region, in which we are interested). In principle, we can

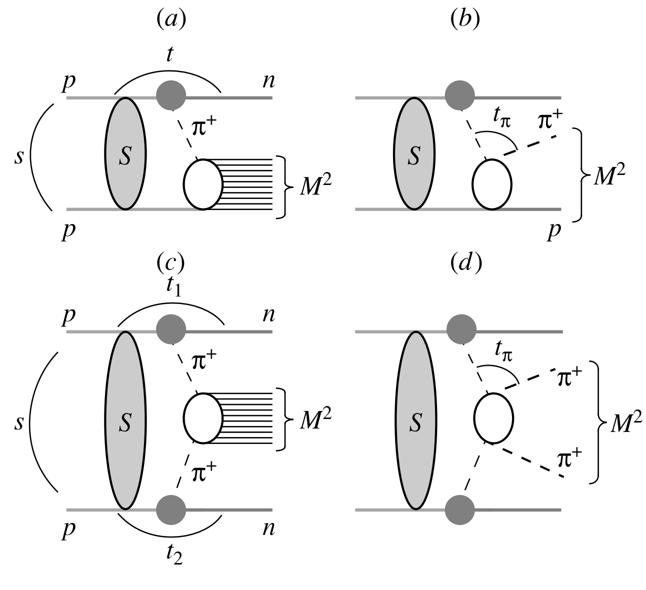

Fig. 1. Diagrams for the processes being considered and kinematical invariants: (a) single pion exchange (SπE) for the case of the total pion–proton cross sections, (b) single pion exchange for the case of the elastic pion–proton cross sections, (c) double pion exchange (DπE) for the case of the total pion–pion cross sections, and (d) double pion exchange with the elastic pion–pion cross sections.

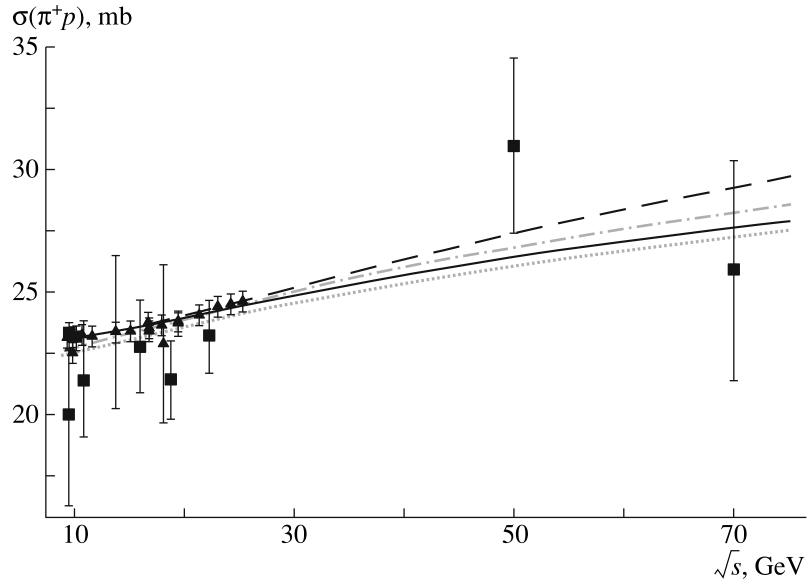

Fig. 2. Direct low-energy data on the total pion–proton cross sections (▲) and data extracted from single pion exchange (■, $\sqrt{s} = 50$ [27], 70 [11], and <25 GeV [11]). The displayed curves represent four parametrizations from [17–21]: (dashed curve) COMPETE [18], (dash-dotted curve) Godizov–Petrov [20, 21], (solid curve) Donnachie–Landshoff [17], and (dotted curve) Bourrely–Soffer–Wu [19].

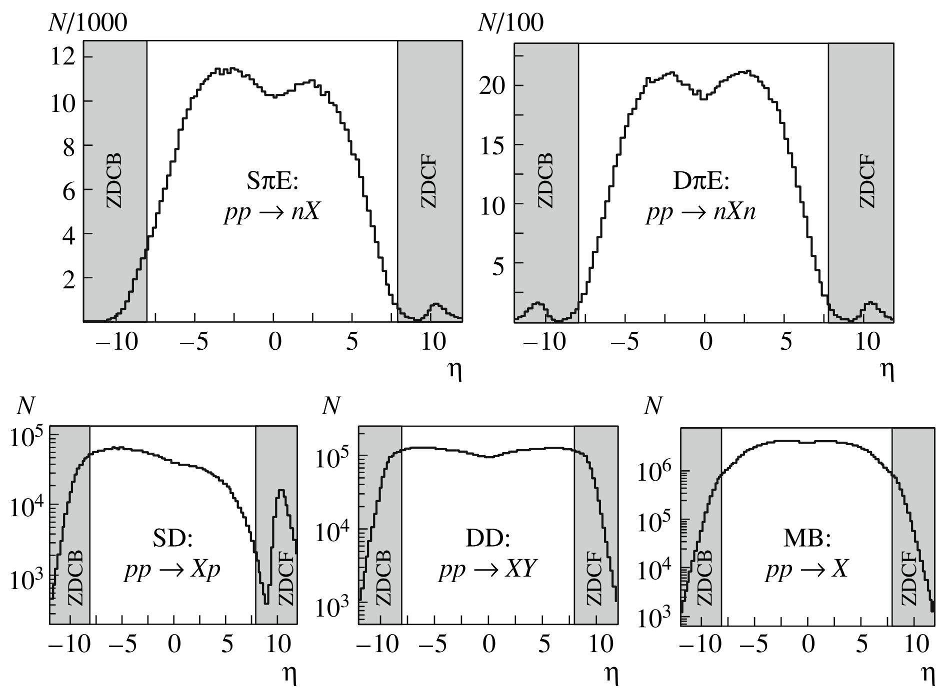

Fig. 3. Pseudorapidity distributions of events for SπE (single pion exchange), DπE (double pion exchange), SD (single diffraction), DD (double diffraction), and MB (minimum bias). The shaded areas correspond to the regions covered by forward and backward ZDC.

also use different models to estimate rescattering—for example, those that were described in [23, 24]. In the ensuing analysis, the following fact is of importance for us: in the physical region of reasonably small values of t, the factors S and S_2 are close to unity; also, they tend to unity in the unphysical region for $t \to m_\pi^2$.

The question of how precisely one can extract the pion–proton and pion–pion cross sections is quite reasonable here. A procedure similar to the Chew–Low method [25, 26] is described in [11]. In order

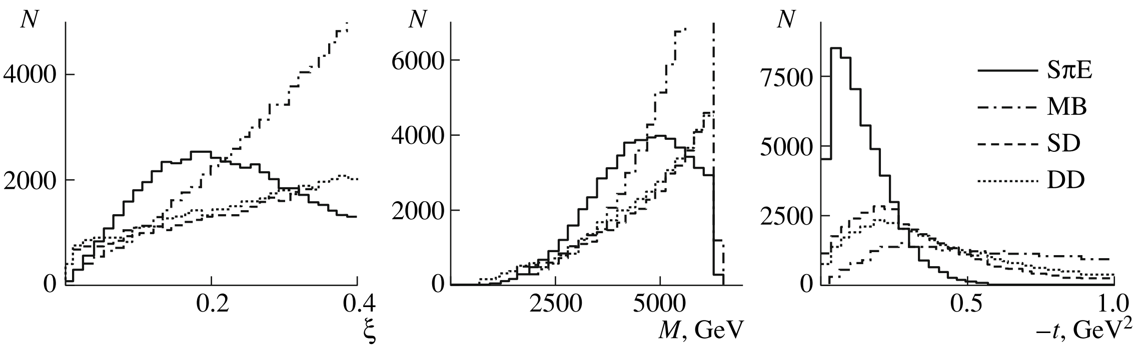

Fig. 4. Distributions of signal and background events with respect to the variables ξ, M, and t for SπE in the case of the total pion–proton cross sections.

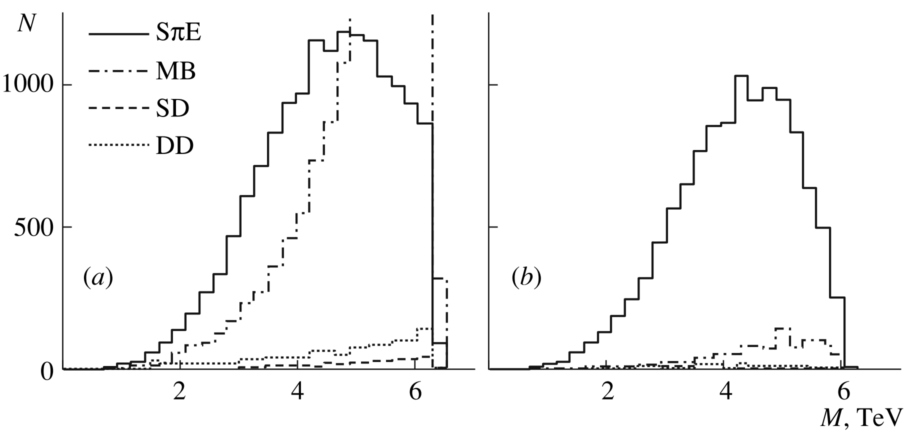

Fig. 5. Distribution of signal and background events for SπE in the case of the total pion–proton cross sections with respect to the variable M for additional selections requiring more than seven hits in HF (a) and after additionally imposing the cut $|t| < 0.2$ GeV^2 (b).

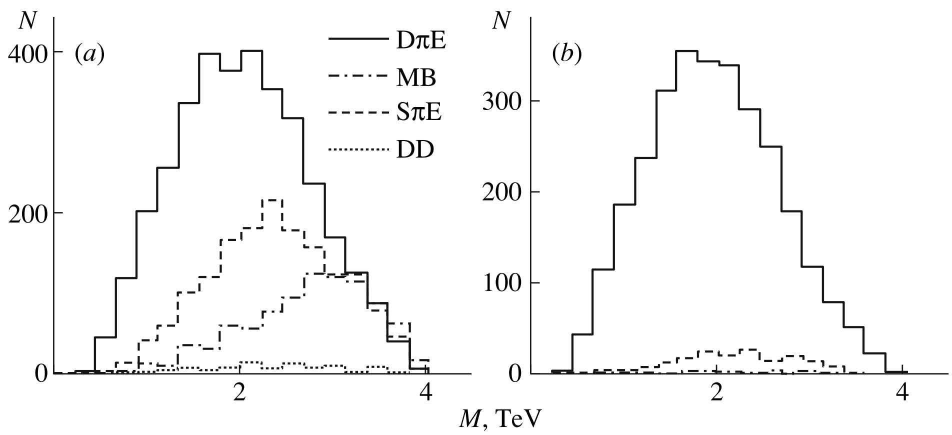

Fig. 6. Distribution of signal and background events for DπE in the case of the total pion–pion cross sections with respect to the variable M for additional selections requiring more than seven hits in HF (a) and after additionally imposing the cut $|t_{1,2}| < 0.3$ GeV^2 (b).

to obtain realistic estimates, we will need a good parametrization of data on the cross sections for single and double pion exchanges in the small-t region. We then take the ratio of these cross sections and the factors appearing in the brackets on the right-hand sides of Eqs. (1) and (2). In an ideal case, we must extrapolate the data to the unphysical region $t \to m_\pi^2$, whereupon $S \equiv S_2 \equiv 1$. We then obtain a model-

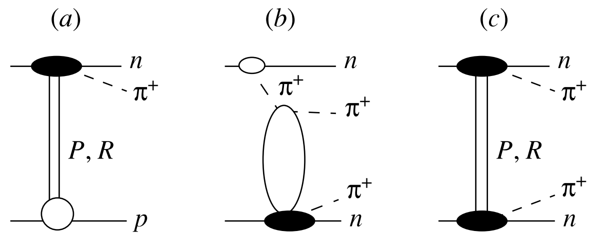

Fig. 7. Exclusive backgrounds to elastic SπE and DπE: (a) single dissociation (background to elastic SπE), (b) process involving single dissociation in the pion–proton channel, and (c) double dissociation (backgrounds to elastic DπE).

independent extraction of the pion–proton and pion–pion cross sections. The experimental situation is much more intricate, as will be seen from the results of a Monte Carlo simulation.

Strictly speaking, we extract cross sections for the scattering of virtual pions having spacelike momenta. However, a decrease in the differential cross sections with increasing t is so fast that a dominant contribution comes from the region $|t| < 0.1$ GeV^2. At such values, the t dependence of the cross sections for π^+p and $\pi^+\pi^+$ scattering can be disregarded. In [11], the total cross section for π^+p scattering was extracted at small values of the variables t and ξ in the physical region from experimental data at low energies [27–30]. The results of applying this procedure are presented in Fig. 2. One can see that the extracted cross sections are close to real experimental data and that the last two points at the energies of 50 and 70 GeV agree well with the parametrizations of the total cross sections. A similar method was used in [31] to extract the pion–pion cross sections in exclusive processes at low energies.

The cross sections for the processes under study are quite large. In the kinematical region specified by the inequalities $|t| < 0.5$ GeV^2 and $\xi < 0.4$, which is studied here, the integrated cross sections have values of about 2 mb (total SπE), 200 μb (total DπE), 266 μb (elastic SπE), and 27 μb (elastic DπE). Therefore, the project under discussion is aimed at studying charge exchanges at early stages of LHC operation or in specific low-luminosity runs in order to avoid dealing with pileup events.

2.2. Monte Carlo Simulation

In order to study experimental possibilities, we have performed a Monte Carlo simulation (at the generator level at the present stage). We have studied basic backgrounds to single and double pion exchanges [single and double diffraction, as well as minimum bias (MB)]. The cross sections and pseudorapidity distributions are presented in Fig. 3. All of the processes involve the production of leading neutrons of pseudorapidity in the region $\eta_n > 8.5$. In order to detect the neutrons, it is proposed to use ZDC (Zero Degree Calorimeter) [32].

Let us consider single-pion exchange for the case where one extracts the total cross section for π^+p scattering. The distributions with respect to various variables of signal and background events are shown in Fig. 4 for $\xi < 0.4$. Without any selections, the signal-to-background ratio is $S/B \sim 1/28$. If we have a ZDC signal on only one side, then the signal-to-background ratio is $S/B \sim 1/2.7$. If one additionally employs the CMS detectors—for example, one takes more than seven hits in HF (Hadronic Forward Calorimeter)—it is possible to improve the signal-to-background ratio to $S/B \sim 1/0.56$ (see Fig. 5). Since background and signal events have different t distributions, we can impose the cut $|t| < 0.2$ GeV^2, in which case $S/B \sim 1/0.08$ (see Fig. 5b). For the present-day structure of ZDC, one can guarantee a cut on t only at a level of 1 GeV^2, but this is insufficient for the proposed measurements. Nevertheless, subsequent investigations revealed that the use of signals from all CMS detectors can make it possible to push the value of S/B up to 2 or 3.

A similar situation prevails for double-pion exchange in the case where one extracts the total cross sections for $\pi^+\pi^+$ scattering. Without selections, the signal-to-background ratio is $S/B \sim 1/380$; upon requiring the presence of signals in both ZDC, we have $S/B \sim 1/1.6$, while, upon additionally requiring more than seven hits in both HF, the signal-to-background ratio becomes $S/B \sim 1/0.7$ (see Fig. 6), which value can be improved by one order of magnitude by imposing the cut $|t_{1,2}| < 0.3$ GeV^2.

In studying the extraction of elastic pion–proton and pion–pion cross sections, we are dealing with the exclusive processes $p + p \to n + \pi^+ + \pi^+ + n$ and $p + p \to p + \pi^+ + n$; therefore, it is necessary to detect final-state pions. The details of this procedure have yet to be clarified conclusively. At the present time, we can state the following:

(i) In the case of SπE without selections, we have $S/B \sim 0.05$; if one additionally requires the absence of signals in all other CMS detectors (Barrel, Endcap, HF, CASTOR, EZDC), $S/B \sim 0.9$ (in this case, there remains the background shown in Fig. 7a); upon subsequently imposing the cut $|t| < 0.2$ GeV^2, we arrive at $S/B \sim 1.7$, while, upon including the selection $|\eta_\pi| > 9$, we have $S/B \sim 5.3$ (see Fig. 8). Having the veto $|\eta_\pi| > 9$ without a cut on t, we can reach a signal-to-background ratio of about several units.

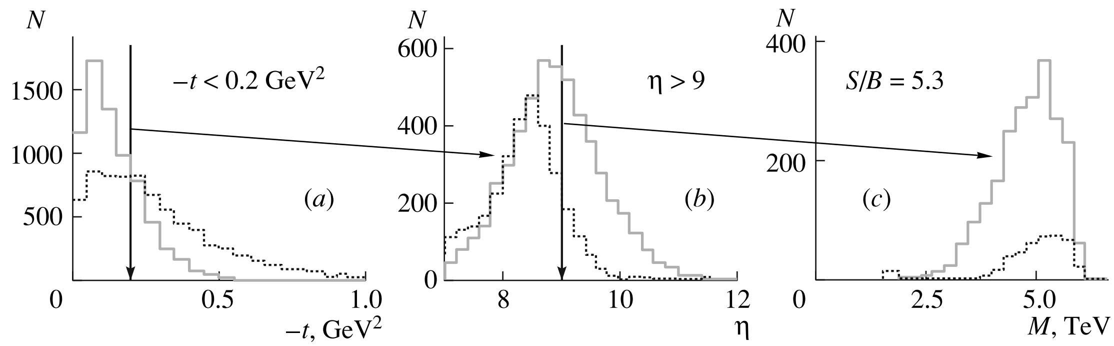

Fig. 8. Successive selections in studying the ratio of the signal (solid-line histogram) to the background (dotted-line histogram) for elastic SπE: (a) t distribution for the case where there is a signal in one of ZDC and where there are no signals in all other CMS detectors on the side of actuated ZDC, (b) pseudorapidity distribution upon imposing the additional cut $|t| < 0.2$ GeV^2, and (c) M distribution upon imposing the additional cut $\eta > 9$ and ultimate signal-to-background ratio.

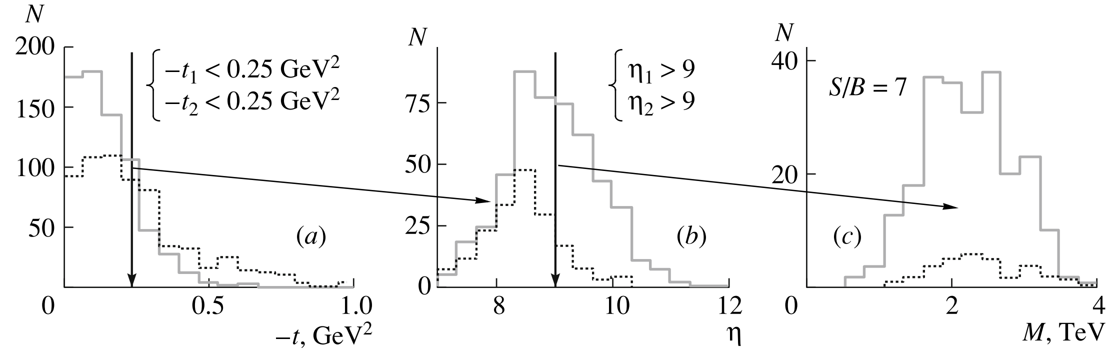

Fig. 9. Successive selections in studying the ratio of the signal (solid-line histogram) to the background (dotted-line histogram) for elastic DπE: (a) distribution with respect to one of $t_{1,2}$ in the case where there are signals in both ZDC and where there are no signals in all other CMS detectors, (b) distribution with respect to one of the pseudorapidities $\eta_{1,2}$ upon imposing the additional cut $|t_{1,2}| < 0.25$ GeV^2, and (c) distribution with respect to M upon imposing the additional cut $\eta_{1,2} > 9$ and ultimate signal-to-background ratio.

(ii) For DπE without selections, the signal-to-background ratio is $S/B \sim 0.04$; the additional requirement of the absence of signals in all other CMS detectors (Barrel, Endcap, HF, CASTOR, EZDC) leads to $S/B \sim 1.1$ (in this case, there remain the backgrounds shown in Figs. 7b and 7c), and the signal-to-background ratio becomes $S/B \sim 2.1$ after subsequently imposing the cut $|t| < 0.25$ GeV^2 (see Fig. 9). The cut $|\eta_\pi| > 9$ leads to the same consequences as in the case of SπE—we then have $S/B \sim 7$.

3. CONCLUSIONS

The present study, proposes an experiment at LHC that would involve detecting leading neutrons. It this experiment, it would be possible to extract the cross sections for π^+p and $\pi^+\pi^+$ scattering at energies of several TeV units. The procedure for extracting cross sections was tested by applying it to low-energy data on single charge exchange. Agreement of extracted cross sections with real experimental data and with parametrizations in the region where there are no experimental data suggests the viability of the proposed method.

Rather accurate measurements of t distributions are of importance for obtaining the pion–proton and pion–pion cross sections since we use an extrapolation. Presently, the structure of the ZDC detectors gives no way to reach the required degree of precision. Only a model-dependent extraction of the cross sections (we mean here models for absorptive corrections) from the charge-exchange cross sections integrated with respect to t is possible at this stage. In order to improve the potential for measurements of neutron transverse momenta, it is proposed to upgrade ZDC by replacing the fiber layers of its hadronic part by THGEM planes, which were developed at the Institute for High Physics (IHEP, Protvino, Russia) [33, 34]. The dimensions of the holes and the distances between them are smaller than 1 mm, and this makes it possible to attain the required precision of measurements in t. The low cost of production, a fast operation, a high radiation strength, and the possibility of measuring the energies and coordinates (transverse momenta) are advantages of such detectors. In conclusion, it is worth emphasizing once again that the derivation of pion–proton and pion–pion cross sections in the TeV energy region is a problem of fundamental importance. The physics potential of such measurements justifies the need for solving challenging technical problems.

ACKNOWLEDGMENTS

This work was supported by the Russian Foundation for Basic Research (project no. 08-02-00405-a).

REFERENCES

1. M. M. Obertino and F. T. S. Araujo, CMS-AN-2008/059.
2. A. Bodek, P. de Barbaro, Y. Chung, et al., CMS-AN-2007/033.
3. M. Pioppi, CMS-AN-2007/032.
4. S. Cerci and D. d'Enterria, CMS-AN-2008/060.
5. V. Petrov, R. Ryutin, and A. Sobol', in *Voyage to the Heart of Matter. 21st Century Physics as Viewed by the Builders of the Experimental Complex at the Large Hadron Collider in Geneva* (Eterna, Moscow, 2009) [in Russian].
6. V. A. Petrov and R. A. Ryutin, J. High Energy Phys. **0408**, 013 (2004).
7. V. A. Petrov, R. A. Ryutin, A. E. Sobol, and J.-P. Guillaud, J. High Energy Phys. **0506**, 007 (2005).
8. A. V. Kisselev, V. A. Petrov, and R. A. Ryutin, Phys. Lett. B **630**, 100 (2005).
9. V. A. Petrov and R. A. Ryutin, J. Phys. G **35**, 065004 (2008).
10. V. A. Petrov, R. A. Ryutin, A. E. Sobol, and J.-P. Guillaud, arXiv:0711.1794 [hep-ph].
11. V. A. Petrov, R. A. Ryutin, and A. E. Sobol, Eur. Phys. J. C **65**, 637 (2010).
12. B. Kopeliovich, B. Povh, and I. Potashnikova, Z. Phys. C **73**, 125 (1996).
13. V. Stocks, R. Timmermans, and J. J. de Swart, Phys. Rev. C **47**, 512 (1993); R. A. Arndt, I. I. Strakovsky, R. L. Workman, and M. M. Pavan, Phys. Rev. C **52**, 2120 (1995).
14. ZEUS Collab (.S. Chekanov et al.), Nucl. Phys. B **637**, 3 (2002).
15. K. G. Boreskov, A. B. Kaidalov, and L. A. Ponomarev, Yad. Fiz. **19**, 1103 (1974) [Sov. J. Nucl. Phys. **19**, 565 (1974)].
16. K. G. Boreskov, A. B. Kaidalov, V. I. Lisin, et al., Yad. Fiz. **15**, 361 (1974) [Sov. J. Nucl. Phys. **15**, 203 (1972)].
17. A. Donnachie and P. V. Landshoff, Phys. Lett. B **296**, 227 (1992).
18. COMPETE Collab. (B. Nicolescu et al.), hep-ph/0110170.
19. C. Bourrely, J. Soffer, and T. T. Wu, Eur. Phys. J. C **28**, 97 (2003).
20. A. A. Godizov and V. A. Petrov, J. High Energy Phys. **0707**, 083 (2007).
21. A. A. Godizov, Yad. Fiz. **71**, 1822 (2008) [Phys. At. Nucl. **71**, 1792 (2008)].
22. V. A. Petrov and A. V. Prokudin, Eur. Phys. J. C **23**, 135 (2002).
23. B. Z. Kopeliovich, I. K. Potashnikova, I. Schmidt, and J. Soffer, Phys. Rev. D **78**, 014031 (2008).
24. B. Z. Kopeliovich, I. K. Potashnikova, I. Schmidt, and J. Soffer, AIP Conf. Proc. **1056**, 199 (2008).
25. G. F. Chew and F. E. Low, Phys. Rev. **113**, 1640 (1959).
26. C. Goebel, Phys. Rev. Lett. **1**, 337 (1958).
27. ZEUS Collab. (J. Breitweg et al.), Eur. Phys. J. C **2**, 247 (1998).
28. W. Flauger and F. Monnig, Nucl. Phys. B **109**, 347 (1976).
29. NA49 Collab. (D. Vagra et al.), Eur. Phys. J. C **33**, S515 (2004).
30. M. Togawa (for the PHENIX Collab.), in *Proc. of the Hamburg 2007, Blois07, Forward Physics and QCD*, p. 308.
31. W. J. Robertson, W. D. Walker, and J. L. Davis, Phys. Rev. D **7**, 2554 (1973).
32. A. S. Ayan et al., CMS-IN-2006/54.
33. Nucl. Instrum. Methods Phys. Res. A **598**, 107 (2009).
34. V. Inshakov et al., arXiv: 0906.4441 [physics.ins-det].

Translated by A. Isaakyan